fluctuation may play an important role in the low-energy charge and spin dynamics, at least in this class of high-T_c cuprates.

References and Notes

1. J. M. Tranquada, B. J. Stemlieb, J. D. Axe, Y. Nakamura, S. Uchida, *Nature* **375**, 561 (1995); J. M. Tranquada *et al., Phys. Rev. B* **54**, 7489 (1996).
2. M. K. Crawford *et al., Phys. Rev. B* **44**, 7749 (1991).
3. J. M. Tranquada *et al., Phys. Rev. Lett.* **78**, 338 (1997); J. M. Tranquada, N. Ichikawa, S. Uchida, unpublished data.
4. S-W. Cheong *et al., Phys. Rev. Lett.* **67**, 1791 (1991); T. E. Mason *et al., ibid.* **71**, 919 (1993); K. Yamada *et al., Phys. Rev. B* **57**, 6165 (1998).
5. H. A. Mook *et al., Nature* **395**, 580 (1998).
6. H. A. Mook, F. Doğan, B. C. Chakoumakos, preprint available at http://xxx.lanl.gov/abs/cond-mat/9811100.
7. J. Zaanen and O. Gunnarsson, *Phys. Rev. B* **40**, 7391 (1989); K. Machida, *Phys. C* **158**, 192 (1989); V. J. Emery and S. A. Kivelson, *ibid.* **209**, 597 (1993).
8. A. H. Castro Neto, *Phys. Rev. Lett.* **78**, 3931 (1997); S. A. Kivelson, E. Fradkin, V. J. Emery, *Nature* **393**, 550 (1998).
9. M. v. Zimmermann *et al., Europhys. Lett.* **41**, 629 (1998); T. Niemöller *et al.*, preprint available at http://xxx.lanl.gov/abs/cond-mat/9904383.
10. Y. Nakamura and S. Uchida, *Phys. Rev. B* **46**, 5841 (1992).
11. M. Hüker *et al., J. Phys. Chem. Solids* **59**, 1821 (1998).
12. S. Tajima *et al., ibid.*, p. 2015.
13. P. M. Singer, A. W. Hunt, T. Imai, preprint available at http://xxx.lanl.gov/abs/cond-mat/9906140.
14. B. Büchner, M. Breurer, A. Freimuth, A. P. Kampf, *Phys. Rev. Lett.* **73**, 1841 (1994).
15. Another advantage we have expected is that we may increase the stability (or pinning strength) of the spin-charge order by using more Nd. Also, we suspect that we have suppressed T_c more to enable the measurements of transport properties to be extended to lower temperatures.
16. Y. Nakamura and S. Uchida, *Phys. Rev. B* **47**, 8369 (1993).
17. As for the superconductivity in the ordered phase, T_c values for all values of x are less than 1.8 K, as estimated by magnetic susceptibility measurements. Apparent T_c at higher temperatures for $x = 0.10$ and $x = 0.15$ presumably comes from a slight inhomogeneity in Nd composition in a crystal.
18. S-W. Cheong *et al., Phys. Rev. B* **49**, 7088 (1994).
19. H. Kuwahara *et al., Science* **272**, 80 (1996).
20. Y. Ando, G. S. Boebinger, A. Passner, T. Kimura, K. Kishio, *Phys. Rev. Lett.* **75**, 4662 (1995); G. S. Boebinger *et al., ibid.* **77**, 5417 (1996).
21. We could not reliably measure R_H at low temperatures because the measurement of R_H has been hindered by the small superconducting signal within the samples, which produces an extra voltage change caused by the magnetic field.
22. M. Sera *et al., Solid State Commun.* **69**, 851 (1989).
23. Use of other data, such as those from neutron diffraction experiments, does not result in any difference in our analysis. In addition, the difference in Nd composition does not affect our conclusion; we reached the same conclusion with $y = 0.4$ data for σ_{xx} and σ_{xy}.
24. It should be noted that R_H is not a truly macroscopic measure of the one-dimensionality of the system. The disappearance of R_H would be realized if the length scale of the 1D segments was larger than the characteristic length scales for one-dimensionality, such as magnetic length or the mean free path.
25. We think longitudinal transport to the stripe direction is more conductive than transverse transport. However, we cannot rule out the possibility that charges are more mobile in the transverse direction (J. Zaanen, personal communication).
26. H. Eskes, O. Y. Osman, R. Grimberg, W. v. Saarloos, J. Zaanen, *Phys. Rev. B* **58**, 6963 (1998).
27. A similar picture is proposed and discussed theoretically in (*8*), where "dynamic" stripes, which interact with each other, are discussed.
28. T. Suzuki *et al., Phys. Rev. B* **57**, 3229 (1998); H. Kimura *et al., ibid.* **59**, 6517 (1999).
29. A. W. Hunt, P. M. Singer, K. R. Thurber, T. Imai, *Phys. Rev. Lett.* **82**, 4300 (1999).

30. Supported by a Grant-in-Aid for Scientific Research and a COE grant from the Ministry of Education, Japan. We acknowledge useful discussions with A. Fujimori, K. Hirota, N. Ichikawa, T. Imai, A. Ino, K. M. Kojima, A. Maeda, N. Nagaosa, S. Tajima, J. M. Tranquada, K. Yamada, and J. Zaanen.

19 May 1999; accepted 18 August 1999

One-Dimensional Electronic Structure and Suppression of *d*-Wave Node State in $(La_{1.28}Nd_{0.6}Sr_{0.12})CuO_4$

X. J. Zhou,[1,2] P. Bogdanov,[1] S. A. Kellar,[1] T. Noda,[3] H. Eisaki,[3] S. Uchida,[3] Z. Hussain,[2] Z.-X. Shen[1]*

Angle-resolved photoemission spectroscopy was carried out on $(La_{1.28}Nd_{0.6}Sr_{0.12})CuO_4$, a model system of the charge- and spin-ordered state, or stripe phase. The electronic structure contains characteristic features consistent with other cuprates, such as the flat band at low energy near the Brillouin zone face. However, the low-energy excitation near the expected *d*-wave node region is strongly suppressed. The frequency-integrated spectral weight is confined inside one-dimensional segments in the momentum space (defined by horizontal momenta $|k_x| = \pi/4$ and vertical momenta $|k_y| = \pi/4$), deviating strongly from the more rounded Fermi surface expected from band calculations. This departure from the two-dimensional Fermi surface persists to a very high energy scale. These results provide important information for establishing a theory to understand the charge and spin ordering in cuprates and their relation with high-temperature superconductivity.

The stripe phase (*1*, *2*), which has attracted considerable attention in connection with recent neutron-scattering data from Nd-substituted $(La_{1.48}Nd_{0.4}Sr_{0.12})CuO_4$ (Nd-LSCO) (*3*), represents a new paradigm for thinking about charge carriers in a solid. Unlike conventional metals in which the charge distribution is homogeneous, the stripe picture asserts that the charge carriers are segregated into one-dimensional (1D) domain walls. At the same time, the electronic spins in the domain between the walls order antiferromagnetically with a π phase shift across the domain wall. The possibility of charge segregation propensity and its implications on conduction as well as superconducting mechanism are at the heart of the current debate in high-temperature superconductivity research (*1*–*24*). Within the context of stripe picture, it is a formidable task to develop a theory describing the electronic structure that provides the microscopic foundation to understand the physical properties. The difficulty stems from the fact that our theoretical machineries are developed either in real space or in momentum (k) space. For an inhomogeneous system like the charge-ordered state, a hybrid description appears to be necessary. This is even more difficult when the strong many-body effects have to be taken into account. So far, little information about the electronic structure of the stripe phase is available. In this report, angle-resolved photoemission data are reported for Nd-LSCO, a model compound for which the evidence for spin and charge ordering is the strongest (*3*). We discuss these results both in terms of the k-space language, which is commonly used to describe the electronic structure of solids, and in terms of a hybrid of the real space and k-space picture. These results may provide a phenomenological foundation to build a comprehensive theory on the charge and spin ordering in cuprates and their relation with superconductivity.

Angle-resolved photoemission spectroscopy (ARPES) measures the single-particle spectral function $A(k, \omega)$ weighted by the photoionization cross section (*25*). Typical spectra of Nd-LSCO (Fig. 1) were sampled from the first and fourth quadrants of the Brillouin zone (BZ) at a temperature of 20 K (*26*). Although the spectra do not contain sharp peak structure, the data still show edge or cusplike structures with clear

[1]Department of Physics, Applied Physics and Stanford Synchrotron Radiation Laboratory, Stanford University, Stanford, CA 94305, USA. [2]Advanced Light Source, Lawrence Berkeley National Lab, Berkeley, CA 94720, USA. [3]Department of Superconductivity, University of Tokyo, Yayoi 2-11-16, Bunkyo-ku, Tokyo 133, Japan.

*To whom correspondence should be addressed. E-mail: zxshen@stanford.edu

angular dependence. As seen in Fig. 1, A to F, with k_x varying from 0.10π to 1.17π (the unit of the momentum is $1/a$ with a being the lattice constant), a broad feature moves from 200 meV or deeper toward the Fermi level E_F and stays there in an extended region near $k_x = \pi$. This dispersion, as well as a strong angular dependence of the spectral weight described below, indicates that the absence of well-defined peaks is not a consequence of random disorder or a poorly cleaved surface. This conclusion is also consistent with the observed low-energy electron diffraction (LEED) pattern.

In the spectral intensity plot (Fig. 2), integrated over a 500-meV energy window of the Fermi level, Fig. 2A shows the raw data and Fig. 2B gives the four-fold symmetrized data. This symmetrization is justified because, in a separate data set that covers the whole quadrant, we did observe high spectral intensity near $(\pi,0)$ and $(0,\pi)$, making the data nearly symmetric with respect to the (0,0)-(π,π) line. The spectral weight, when integrated over a large frequency window, represents the momentum distribution function $n(k) = \int_{-\infty}^{+\infty} A(k,\omega) f(\omega) d\omega$ weighted by the photoionization cross section. The k dependence is very clear in the momentum distribution function, lending strong support for the k-resolved nature of the data even though the features are not very sharp in energy. The high $n(k)$ area is approximately confined within 1D segments with the range of $|k_x| \leq \pi/4$ for any k_y or $|k_y| \leq \pi/4$ for any k_x (Fig. 2B). On the other hand, the low-energy spectral weight (Fig. 3) is mostly concentrated near the $(\pi,0)$ region. It is also striking that there is little or no low-energy spectral weight near the zone diagonal [(0,0) to (π,π) direction], where the d-wave gap has nodes. Usually, in cuprate superconductors, there is clear dispersion along (0,0) to (π,π) with a Fermi crossing near $(\pi/2,\pi/2)$; this is the node region where the d-wave superconducting gap is zero. The absence of such a Fermi crossing in Nd-LSCO can be best illustrated by the absence of any dispersive feature for the $k_y = 0.44\pi$ cut (Fig. 1I), indicating that the usual Fermi surface near the d-wave node region is very poorly defined.

In general, the $n(k)$ pattern allows one to determine the underlying Fermi surface that separates the occupied area from the unoccupied area (*27*). There are two possible ways to think about the data that are consistent with charge density modulations, albeit at very different limits. In the limit for which the charge density modulation is weak, a two-dimensional (2D) interpretation of the data is probably a reasonable starting point. The Fermi surface determined is approximately the lines of $k_x = \pm \pi/4$ or $k_y = \pm \pi/4$, as depicted in Fig. 2C. Counting the occupied area of the BZ, one gets 7/16, or 1/16 short of 1/2 of a BZ area. With the spin degeneracy, this is consistent with the 1/8 doping of the system. The shape of the Fermi surface has some qualitative resemblance to

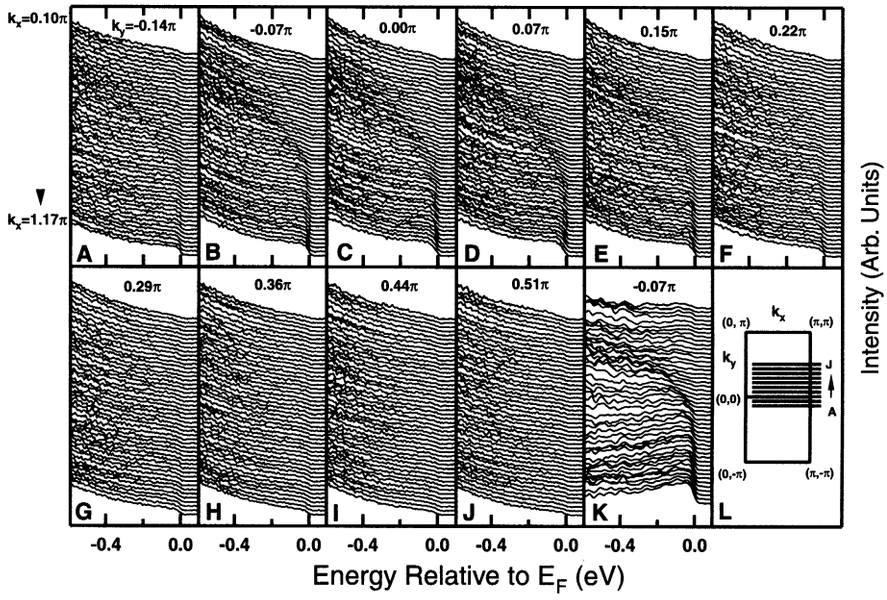

Fig. 1. Angle-resolved photoemission spectra taken on Nd-LSCO at 20 K. The measurement scheme is depicted in (**L**), which covers the first and fourth quadrants. Each of the panels (**A**) to (**J**) represents a cut parallel to the (0,0) to $(\pi,0)$ direction with k_x covering from 0.10π to 1.17π with an interval of 0.023π. (A) to (J) cover k_y from -0.14π to 0.51π with an interval of 0.07π. (**K**) shows the same spectra as in (B), but with the high-energy background removed.

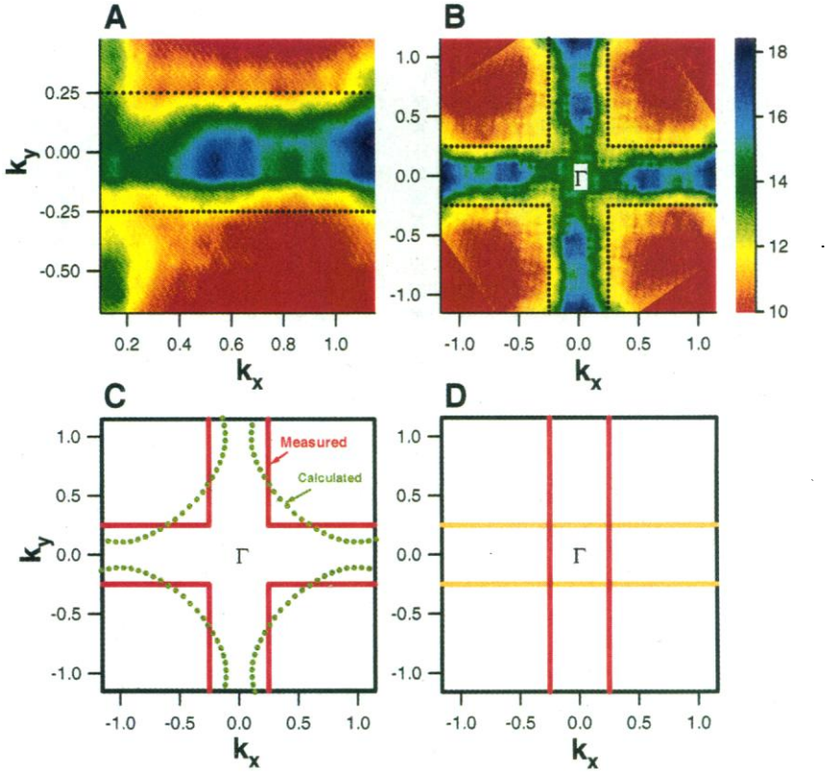

Fig. 2. Spectral weight integrated within 500 meV of the Fermi level, as a function of k_x and k_y. (**A**) is obtained directly from the raw data, whereas (**B**) is obtained by symmetrizing (A) with four-fold symmetry. The dotted lines in (A) and (B) define the regions where the spectral weight is mainly concentrated. (**C**) depicts the underlying Fermi surface (solid line) obtained from (B) that encloses the high spectral weight region. The calculated Fermi surface for the 2D CuO_2 plane (*28*) is also shown (dotted lines) for comparison. (**D**) depicts the Fermi surface expected from two perpendicular 1D stripe domains in the 1D interpretation. Γ is the center of the BZ.

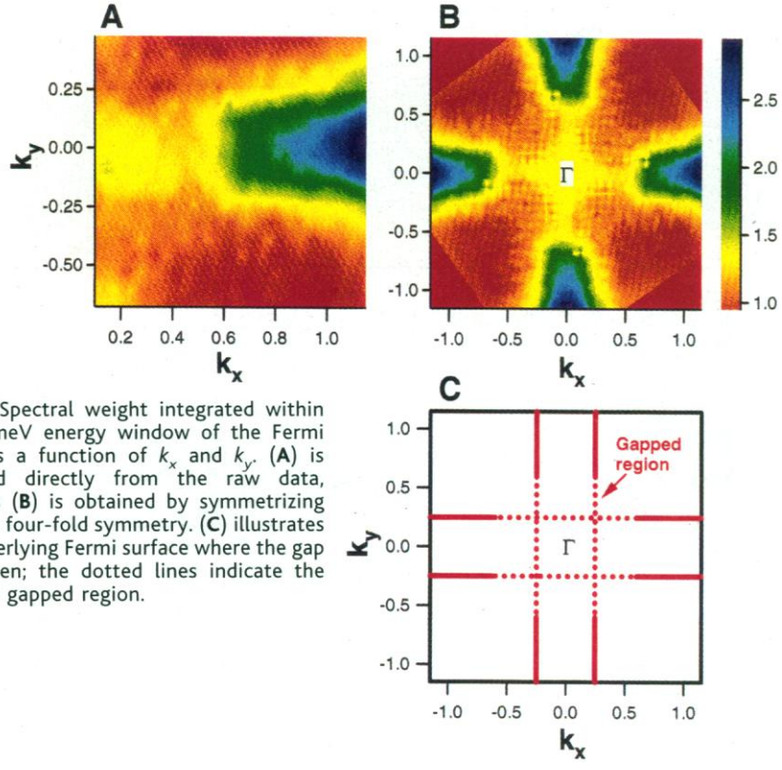

Fig. 3. Spectral weight integrated within a 100-meV energy window of the Fermi level, as a function of k_x and k_y. (**A**) is obtained directly from the raw data, whereas (**B**) is obtained by symmetrizing (A) with four-fold symmetry. (**C**) illustrates the underlying Fermi surface where the gap may open; the dotted lines indicate the possible gapped region.

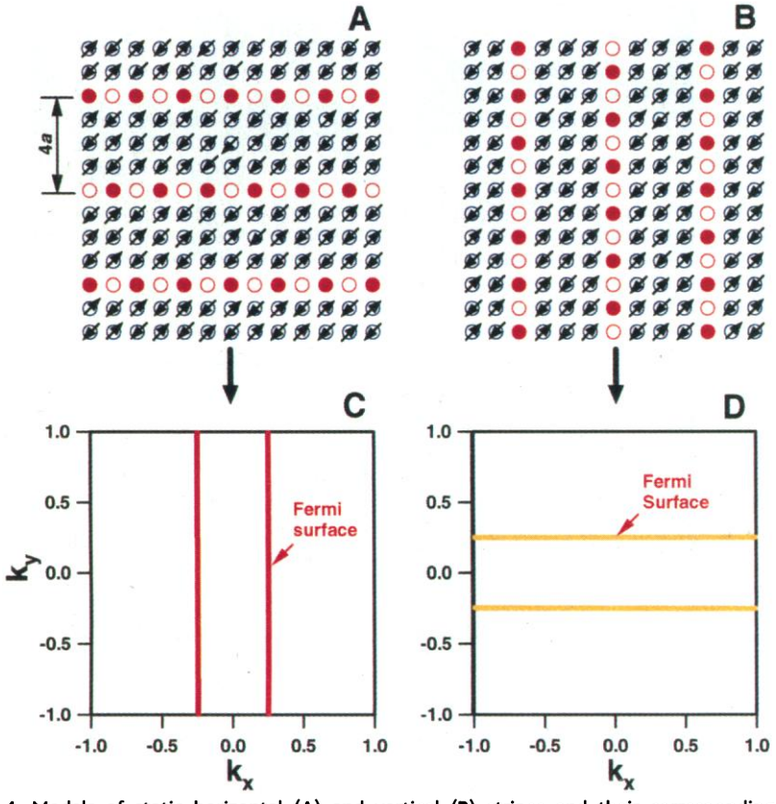

Fig. 4. Models of static horizontal (**A**) and vertical (**B**) stripes and their corresponding Fermi surfaces. The horizontal stripe (A) is expected to result in the Fermi surface defined by the lines $|k_x| = \pi/4$ (**C**), whereas the vertical stripe (B) results in the Fermi surface defined by the lines $|k_y| = \pi/4$ (**D**).

what one expects from a band calculation (dotted lines in Fig. 2C) (*28*), although the straight 1D segments are absent in the calculation. In this case, we have almost perfectly nested Fermi surface segments, which would favor a charge-density wave (CDW) instability leading to a quasi-2D picture. Simple geometrical consideration of the crosslike Fermi surface leads to the conclusion that the Fermi surface nesting is commensurate with the lattice at 1/8 doping. Electron-phonon interaction would favor a CDW at this filling level. This is consistent with the fact that 1/8 doping is where most of the anomalies are observed and also that spin-ordering temperature is correlated with structural phase transition (*3*, *29*).

There are serious problems with the above quasi-2D picture for the strongly charge-ordered Nd-LSCO. First, there is no obvious origin for the almost perfectly nested Fermi surface segments. Second, it is unclear why the states near the *d*-wave node are strongly suppressed if the charge modulation is very weak. As shown in Figs. 2 and 3, the suppression of the *d*-wave node state can be thought of as the opening of a large gap (500 meV or beyond) if one insists on the quasi-2D picture. It is difficult to justify the opening of such a large gap with phonons. Furthermore, a CDW would open a gap along the entire nested Fermi surface segments, not preferentially near the *d*-wave node only. Third, the quasi-2D picture is not consistent with the neutron-scattering data in which the two pairs of incommensurate scattering spots are interpreted to be from stripes in two adjacent planes that are rotated by 90° (*3*). In addition, the CDW picture does not have as natural a connection to the spin density wave observed as a stripe picture would.

We now discuss an alternative interpretation, which is consistent with the stripe picture, in terms of a hybrid of the real and *k*-space picture. Here the charge modulation is assumed to be much stronger. It is plausible that the four-fold symmetry seen in our experiments stems from two sets of orthogonal domains as depicted in Fig. 4. At 1/8 doping, neutron- and x-ray–scattering experiments suggest that each charge stripe is separated by three antiferromagnetic lines so the charge has a periodicity of 4*a*, whereas the stripe itself is 1/4 filled (Fig. 4A and B) (*3*, *30*). For each domain, the Fermi surface is either the $k_x = \pm\pi/4$ or $k_y = \pm\pi/4$ lines (Fig. 4, C and D). The stripes along the horizontal direction give rise to the vertical Fermi surface lines of $k_x = \pm \pi/4$. In this context, the Fermi surface observed can be understood as a superposition of two perpendicular Fermi surfaces arising from two different domains (Fig. 2D). The stripe phase contains undoped insulating areas and doped metallic areas. The signal from the insulating areas is pushed to higher binding energy because of the Mott gap; the low-energy feature is thus mainly from the metallic region. A two-com-

ponent electronic state has been observed in $(La_{2-x}Sr_x)CuO_4$ near the metal-insulator transition region of $x \sim 0.05$ to 0.07, consistent with this picture (*31*). With static stripes, one expects this effect to be enhanced in Nd-LSCO. Because the metallic stripes are 1/4 filled at 1/8 doping (*3*), it is consistent with the occupied state being confined within $|k_x| = \pi/4$. In this scenario, there should be a potential between the charge-rich and charge-poor regions.

The above discussion leads to a picture that favors the 1D approach rather than the quasi-2D approach for the electronic structure of Nd-LSCO, although our results alone cannot definitely distinguish between them; the occupied area agrees with the Luttinger volume in both cases. The straight segments seen in the raw data reveal the 1D-like Fermi surface sections that will manifest themselves in transport experiments independent of the interpretation (*29*). How to reconcile the *k*-space picture (Fermi surface, and so forth) and the real space picture (inhomogeneous charge distribution) is a key difficulty in describing the stripe phase. The data can probably provide insight into this problem by providing *k*-space information on the stripe phase. The stripe interpretation has the added advantage of explaining the suppression of the *d*-wave node state (*18*). This is reasonable because the 1D structure of the stripes is not compatible with the 2D character of the *d*-wave state. We note that this is also the case for superconducting $(La_{2-x}Sr_x)CuO_4$ with a similar Sr concentration, for which the spectral weight along the (0,0) to (π,π) direction is strongly suppressed (*31*). This behavior is very different from the pseudogap state seen in underdoped Bi2212 (*32*). In the context of the hybrid picture discussed above, the signal along the zone diagonal is due to states from the insulating regions and is thus pushed to higher energy because of the gap. This also implies that the low-energy state near $(\pi,0)$ stems from the hole-rich region of the stripes (*16*).

It is seen that the dispersion of the broad feature is very similar in Fig. 1, A to F. At higher k_y, the dispersive feature fades away rapidly. To aid in determining the dispersion, we removed the angular independent part of the data, as exemplified in Fig. 1K for $k_y = -0.07\pi$. The momentum dependence (Fig. 5A), determined from the leading edge of the features for $k_y = -0.14\pi$ to 0.15π, shows strong dispersion when k_x is smaller than 0.7π but virtually no dispersion for k_x larger than 0.7π. The dispersionless features near $(\pi,0)$ show a nearly 5-meV or smaller gap with respect to the Fermi level. This behavior is also related to the flat band near $(\pi,0)$, which is universally observed in *p*-type cuprates and may be related to the small velocity scale observed (*33*). The present observation of the flat band in a stripe system suggests an underlying reason for it (*16*). On the other hand, the data show relatively weaker dispersion with k_y as the curves for different k_y fall more or less on the same line within the experimental uncertainty. In the dispersion along k_y (Fig. 5B), for some k_x cuts, such as $k_x = 0.67\pi$, there appears to be some dispersion along k_y, although we caution that the energy position uncertainty is also large.

Intuitively, one may think of strong dispersion with k_x as arising from the horizontal stripes (along the *x* direction). Then the spectral intensity confinement within $k_y = \pm\pi/4$ might be related to the 4*a* charge periodicity along the *y* direction; it would fold the BZ from $k_y = \pm\pi$ to $k_y = \pm\pi/4$. However, with this picture, it is hard to explain why the spectral weight does not repeat in other zones. Moreover, a 1/4-filled horizontal stripe would give a band filled within $k_x = \pm\pi/4$, which is not consistent with the fact that the filled band extends all the way to $(\pi,0)$. The more likely interpretation is that the horizontal spectral weight concentration is from vertical stripes (along the *y* direction). As shown in Fig. 4, the confinement of the spectral weight within $k_y = \pm\pi/4$ can be understood because, for a given k_x, one only sees the occupied band within $k_y \leq \pi/4$ as the vertical stripes are 1/4 filled. This interpretation is further supported by the model calculation, in which the calculated spectral density for the vertical stripes is qualitatively in agreement with the measured spectral confinement near $(\pi,0)$ (Fig. 3A) (*16*). This picture also provides a possible explanation for the two broad intensity maxima in $n(k)$ (Fig. 2A). These two maxima are separated in k_x by about 0.5π, consistent with a real space stripe periodicity of 4*a*.

As depicted in Fig. 3C, the data can be thought of as the opening of an anisotropic gap along the Fermi surface (*34*). As illustrated in Fig. 2, the $|k_x| \cong \pi/4$ or $|k_y| \cong \pi/4$ lines represent the underlying Fermi surface that separates the occupied states from the unoccupied states. The lowest energy excitations along the Fermi surface give the energy gap. Thus, the leading edge position in Fig. 5A is a good representation of the *k* dependence of the gap (*35*). This gap is highly anisotropic and reaches an energy scale up to 200 meV. Although we are not sure about the microscopic origin of the gap, a naive possibility is the 1/4-filling along the 1D stripe, which would give rise to a gap (see the inset of Fig. 5B). The anisotropy stems from the underlying electronic structure of the material.

The data presented in this report seem to present some apparent paradoxes. The persistence of the 1D-like character up to 500 meV or beyond (Fig. 2) is unexpected from theories that start with quasi-particles defined very close to the Fermi energy. From the viewpoint of Fermi

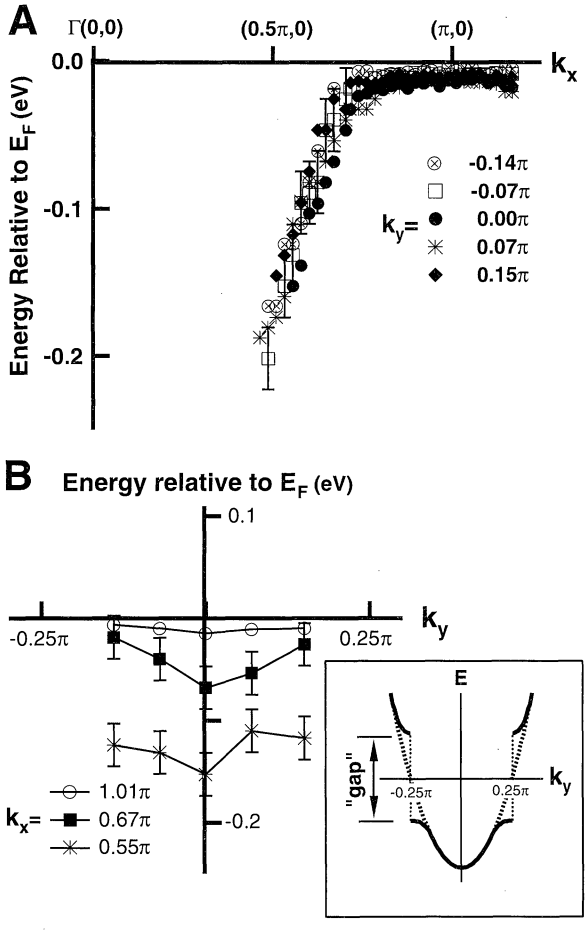

Fig. 5. (A). Dispersion relations obtained from Fig. 1, A to E. For clarity, only the error bar for the $k_y = -0.07\pi$ data is marked. **(B)** Dispersion relation along the k_y direction for three typical k_x. The inset shows schematically the possible opening of a gap at $\pm k_y$ associated with 1/4-filling of the 1D stripe.

liquid plus CDW theory and given the relatively low ordering temperature (~30 to 70 K) (*3, 24, 30*), one would expect 1D behavior only at an energy scale much lower than 500 meV. The solution to this dramatic departure from the Fermi liquid paradigm appears to call for a different basic starting point. Instead of quasiparticles, one may start with stripes that are at least locally stable up to very high energy, as reflected in ARPES data that are mainly sensitive to the local information at such high energy. The fluctuation of the stripes may give rise to the global 2D character in the intermediate energy and temperature scale. The ordering seen in neutron-scattering and nuclear quadrupole resonance (NQR) experiments is the freezing out of these fluctuations (*3, 24*) that results in the long range order. In this sense, one may consider that the ARPES data reflect the local amplitude of stripe formation, which is of high energy scale, whereas the neutron-scattering and NQR data reflect the phase of stripe correlation. This discussion then leads to another paradox, which has to do with the edge dispersion perpendicular to stripes. How can charges, which are already confined to stripes at energy scale of 500 meV, experience perpendicular motion with the dispersion of 200 meV (Fig. 5A)? This may be related to the paradox that the spectra are extremely broad in energy yet sharply defined in momentum, as reflected in the $\pi/4$ boundary separating the high and low spectral weight regions. We have no clear answer, but we speculate that it is related to the fact that stripes tend to be 1/4 filled (*3, 14, 15, 22*) and the stripe fluctuations can give charge motions (coherent or incoherent) perpendicular to stripes. Further theoretical work that takes into account the energetics of charge motion in an antiferromagnetic background and stripe potential (*36*) and investigates the connection of the edge dispersion to the transverse stripe fluctuation (*8–13*) is needed to address these issues.

References and Notes

1. S. A. Kivelson and V. J. Emery, in *Strongly Correlated Electronic Materials: The Los Alamos Symposium 1993*, K. S. Bedell *et al.*, Eds. (Addison-Wesley, Reading, MA, 1994), pp. 619–650; V. J. Emery, S. A. Kivelson, O. Zacher, *Phys. Rev. B* **56**, 6120 (1997).
2. J. Zaanen and O. Gunnarson, *Phys. Rev. B* **40**, 7391 (1989).
3. J. M. Tranquada, B. J. Sternlieb, J. D. Axe, Y. Nakamura, S. Uchida, *Nature* **375**, 561 (1995); J. M. Tranquada, N. Ichikawa, S. Uchida, *Phys. Rev. B* **59**, 14712 (1999).
4. D. Poilbanc and T. M. Rice, *Phys. Rev. B* **39**, 9749 (1989).
5. H. J. Schulz, *J. Phys.* **50**, 2833 (1989).
6. C. Castellani, C. D. Castro, M. Grilli, *Phys. Rev. Lett.* **75**, 4650 (1995).
7. A. H. Castro Neto and D. Hone, *ibid.* **76**, 2165 (1996).
8. J. Zaanen, M. L. Horbach, W. V. Saarloos, *Phys. Rev. B* **53**, 8671 (1996).
9. H. Eskes, R. Grimberg, W. Van Saarloos, J. Zaanen, *ibid.* **54**, R724 (1996); H. Eskes, O. Y. Osman, R. Grimberg, W. V. Saarloos, J. Zaanen, *ibid.* **58**, 6963 (1998).
10. C. Morais Smith, Y. A. Mimashko, N. Hasselmann, A. O. Calderia, *ibid.* **58**, 453 (1998).
11. S. A. Kivelson, E. Fradkin, V. J. Emery, *Nature* **393**, 550 (1998).
12. J. Zaanen, O. Y. Osman, W. Van Saarloos, *Phys. Rev. B* **58**, R11868 (1998).
13. N. Hasselmann, A. H. Castro Neto, C. Morais Smith, Y. Dimashko, *Phys. Rev. Lett.* **82**, 2135 (1999).
14. J. Zaanen and A. M. Oles, *Ann. Phys.* **5**, 224 (1996).
15. C. Nayak and F. Wilczek, *Phys. Rev. Lett.* **78**, 2465 (1997).
16. M. I. Salkola, V. J. Emery, S. A. Kivelson, *ibid.* **77**, 155 (1996).
17. S. R. White and D. J. Scalapino, *ibid.* **81**, 3227 (1998).
18. T. Tohyama, S. Nagai, Y. Shibata, S. Maekawa, *ibid.* **82**, 4910 (1999).
19. A. V. Balatsky and P. Bourges, *ibid.*, p. 5337.
20. B. O. Wells *et al.*, *Science* **277**, 1067 (1997).
21. G. Aeppli *et al.*, *ibid.* **278**, 1432 (1997).
22. K. Yamada *et al.*, *Phys. Rev. B* **57**, 6165 (1998); Y. S. Lee *et al.*, preprint available at xxx.lanl.gov/abs/cond-mat/9902157.
23. H. A. Mook *et al.*, *Nature* **395**, 580 (1998).
24. A. W. Hunt, P. M. Singer, K. R. Thurber, T. Tmai, *Phys. Rev. Lett.* **82**, 4300 (1999).
25. The ARPES data were recorded at the beamline 10.0.1.1 of the Advanced Light Source. Fifty-five–electron volt photon energy was used for more efficient *k*-space sampling. With the use of the angular mode of the Scienta analyzer, the momentum resolution was 0.02π. The energy resolution was detuned from its optimal 7 meV to 16 meV so that a few thousand spectra with sufficient statistics could be obtained during the lifetime of a cleaved surface. For example, the 500 spectra presented in Fig. 1 of this paper were recorded within the first 3 hours after the cleaving; the results are robust from cleave to cleave. The vacuum during the measurement was ~2 to 5×10^{-11} torr. LEED experiments were performed to check the surface structure, yielding the expected four-fold symmetry. The Nd-LSCO sample was grown with the traveling floating zone method. The same class of samples has been used for neutron-scattering experiments (*3*).
26. The angular mode of the analyzer allows us to cover nearly a whole quadrant along k_x with 48 points at the same time, which correspond to the spectra in Fig. 1, A to J; the whole BZ is then measured by taking various k_y cuts.
27. Here the "occupied" area means that the occupation probability is high. In an interacting system, $n(k)$ will not be zero even in the region where the "band" is above the Fermi level.
28. P. H. Dickinson and S. Doniach, *Phys. Rev. B* **47**, 11447 (1993).
29. Y. Nakamura and S. Uchida, *ibid.* **46**, 5841 (1992).
30. M. V. Zimmermann *et al.*, *Europhys. Lett.* **41**, 629 (1998).
31. A. Ino *et al.*, preprint available at xxx.lanl.gov/abs/cond-mat/9809311; A. Ino *et al.*, preprint available at xxx.lanl.gov/abs/cond-mat/9902048.
32. A. G. Loeser *et al.*, *Science* **273**, 325 (1996); D. S. Marshall *et al.*, *Phys. Rev. Lett.* **76**, 4841 (1996); H. Ding *et al.*, *Nature* **382**, 51 (1996).
33. A. V. Balatsky and Z.-X. Shen, *Science* **284**, 1137 (1999).
34. From the outset, we note that this gapping effect is not caused by the extrinsic loss mechanism suggested recently [R. Joynt, *Science* **284**, 777 (1999)], which cannot explain the angular dependence of the gap. In this case, the smallest gap is 5 meV or less, further suggesting that the extrinsic loss mechanism is not an issue here.
35. Although no data for $|k_y| = 0.25\pi$ are available, because the dispersion with k_y is very minimal, the $|k_y| = 0.15\pi$ result is a good indicator of the gap.
36. E. Dagotto, *Rev. Mod. Phys.* **66**, 763 (1994).

37. We thank E. D. Lu, J. Denlinger, J. Bozek, and D. H. Lu for technical support and S. A. Kivelson, J. Zaanen, R. B. Laughlin, D. van der Marel, A. Fujimori, H. Fukuyama, C. D. Castro, W. Hanke, and J. M. Tranquada for helpful comments. The experiment was performed at the Advanced Light Source of the Lawrence Berkeley National Laboratory, which is operated by the U.S. Department of Energy's Office of Basic Energy Science, Division of Material Science. The division also provided support for the Stanford Synchrotron Radiation Laboratory experimental effort and end-station development through grant DE-FG03-96ER45594. The Stanford University work was also supported by NSF grant DMR-9705210.

21 June 1999; accepted 31 August 1999

Evidence of Nonlinear Elasticity of the Crust from the Mw7.6 Manyi (Tibet) Earthquake

Gilles Peltzer,[1]* Frédéric Crampé,[2] Geoffrey King[2]

Satellite synthetic aperture radar (SAR) interferometry shows that the magnitude 7.6 Manyi earthquake of 8 November 1997 produced a 170-kilometer-long surface break with up to 7 meters of left-lateral slip, reactivating a N76°E quaternary fault in western Tibet. The radar interferometric map reveals asymmetric, along-strike displacement profiles between the two sides of the surface rupture, a pattern that cannot be explained with linear elastic theory. This observation suggests that the elastic moduli of the crust in tension and in compression are different because of the presence of cracks in the crust at shallow depth. A model indicates that a ratio of 2 between compressive and tensile elastic moduli can account for the observed asymmetry, a ratio that is consistent with laboratory and borehole measurements.

Geodetic measurements of the static surface displacement field produced by large earthquakes provide information about their source mechanism. Linear models of dislocation in an elastic half-space (*1*) are widely used to represent earthquake faults and generally provide a satisfactory fit to near- and far-field displacement data obtained with conventional geodetic techniques (*2*). However, laboratory experiments and in situ measurements in boreholes have shown that many crustal rocks exhibit a nonlinear elastic behavior in compression and tension with a dependence of the Young's modulus on the minimum principal stress (*3*). The effects of nonlinear elastic properties of crustal rocks

LINKED CITATIONS

One-Dimensional Electronic Structure and Suppression of d-Wave Node State in (La _{1.28} Nd _{0.6} Sr _{0.12})CuO₄

X. J. Zhou; P. Bogdanov; S. A. Kellar; T. Noda; H. Eisaki; S. Uchida; Z. Hussain; Z.-X. Shen

Science, New Series, Vol. 286, No. 5438. (Oct. 8, 1999), pp. 268-272.

References and Notes

[20] **Incommensurate Spin Fluctuations in High-Transition Temperature Superconductors**

B. O. Wells; Y. S. Lee; M. A. Kastner; R. J. Christianson; R. J. Birgeneau; K. Yamada; Y. Endoh; G. Shirane

Science, New Series, Vol. 277, No. 5329. (Aug. 22, 1997), pp. 1067-1071.

Stable URL:
http://links.jstor.org/sici?sici=0036-8075%2819970822%293%3A277%3A5329%3C1067%3AISFIHT%3E2.0.CO%3B2-R

[21] **Nearly Singular Magnetic Fluctuations in the Normal State of a High-T_c Cuprate Superconductor**

G. Aeppli; T. E. Mason; S. M. Hayden; H. A. Mook; J. Kulda

Science, New Series, Vol. 278, No. 5342. (Nov. 21, 1997), pp. 1432-1435.

Stable URL:
http://links.jstor.org/sici?sici=0036-8075%2819971121%293%3A278%3A5342%3C1432%3ANSMFIT%3E2.0.CO%3B2-J

[32] **Excitation Gap in the Normal State of Underdoped Bi₂Sr₂CaCu₂O _{8+δ}**

A. G. Loeser; Z.-X. Shen; D. S. Dessau; D. S. Marshall; C. H. Park; P. Fournier; A. Kapitulnik

Science, New Series, Vol. 273, No. 5273. (Jul. 19, 1996), pp. 325-329.

Stable URL:
http://links.jstor.org/sici?sici=0036-8075%2819960719%293%3A273%3A5273%3C325%3AEGITNS%3E2.0.CO%3B2-B

LINKED CITATIONS

[33] **Is This Why T_c Is So Low?**

A. V. Balatsky; Z.-X. Shen

Science, New Series, Vol. 284, No. 5417. (May 14, 1999), pp. 1137-1138.

Stable URL:

http://links.jstor.org/sici?sici=0036-8075%2819990514%293%3A284%3A5417%3C1137%3AITWTIS%3E2.0.CO%3B2-R

[34] **Pseudogaps and Extrinsic Losses in Photoemission Experiments on Poorly Conducting Solids**

Robert Joynt

Science, New Series, Vol. 284, No. 5415. (Apr. 30, 1999), pp. 777-779.

Stable URL:

http://links.jstor.org/sici?sici=0036-8075%2819990430%293%3A284%3A5415%3C777%3APAELIP%3E2.0.CO%3B2-0